MRS Advances © 2018 Materials Research Society
DOI: 10.1557/adv.2018.434

Visualization of Self-sorted Local Atomic Motifs in disordered solids

Aly Rahemtulla[1], Bruno Tomberli[2] and Stefan Kycia[1]

[1]*Department of Physics, University of Guelph, Guelph, Ontario, Canada*

[2]*Department of Physics, Capilano University, North Vancouver, British Columbia, Canada*

ABSTRACT

The structural descriptions of even the most basic amorphous materials are under considerable debate. In this work, an intuitive computational technique has been developed to construct 3D statistical density maps to directly visualize and identify local atomic structures from simple monatomic amorphous germanium (a-Ge) to complex multi-atom systems such as copper zirconium metallic glass. We show motifs in copper zirconium that are unresolvable through traditional tools such as Voronoi indexing. This self-sorted local atomic motif (SLAM) method builds upon the Kabsch algorithm incorporating techniques in computer vision to produce least-squares optimized 3D density maps. Simultaneously, the SLAM method incorporates self-contained categorization to define local motifs based upon atomic structures. We present the methodology of the SLAM method and also present resulting motifs comparing models a-Ge and demonstrate its broad capability on metallic glass.

INTRODUCTION

The emerging properties of amorphous solids result from their complex, seemingly random arrangements of elements [1]. The resolution of details extracted through experimental methods has improved [2]. The lack of long range ordering in amorphous materials makes resolving amorphous structure through experiment alone a great challenge [3]. Theoretical models have provided many possible solutions for the underlying structures of amorphous solids, from the simple covalent bond networks of amorphous silicon (a-Si) and amorphous germanium (a-Ge) to metallic glasses [4-14]. Computational modelling has grown increasingly robust as technology has steadily improved. Nevertheless, interpreting the short-range order in such models still remains a challenge.

Traditional techniques of structure interpretation aid greatly in identifying crystalline-like motifs [15-17]. However, these one dimensional parameters can lose detailed information consequently limiting their ability to help interpret new structures. Geometric analysis such as Voronoi indexing improves upon this by describing a volumetric shape enclosed by atoms, defining motifs by the types of surfaces enclosing a volume [18, 19]. This approach has limited accuracy and can bias the interpretation [20].

Recent work by Tomberli et al. [21] introduces a different geometric approach called the Local Atomic Motif (LAM) method, with improvements made by Rahemtulla et al. [22]. The LAM approach along with the work of Fang et al. [20] attempt to mitigate the shortcomings in traditional analysis. The atomistic alignments in the latter approach are innovatively resolved using an interatomic potential. However the underlying consequence of this approach requires significant computational resources to perform such alignments and knowledge of the rotational transformation is lost in the process. Both methods additionally lack the means to identify and classify motifs that are not predetermined.

This work introduces the methodology of a Self-sorting Local Atomic Motif (SLAM) method, which builds upon the principle of LAMs but introduces the functionality of self-categorization and a sophisticated alignment process to showcase the representative degree of short-range ordering in atomic models.

METHODS

We develop a method of both producing highly ordered LAMs similar to what was presented through tetrahedral optimizations [22]. However, this new method no longer requires prior knowledge of the structure. This process will also self-categorize the resulting motifs based on least-squares differences in their structure. This SLAM method can be readily applied to any system to help classify all unique motifs present in a model. LAMs of these motifs showcase the degree of order or disorder present.

The SLAM process begins by defining clusters, containing the relative positions of all atoms within a cut-off distance of a central atom for a given model. Each cluster is then compared to existing motifs. If the cluster is similar to a motif, it is aligned to that motif using the Kabsch algorithm [23], which creates a least-squares rotation matrix using singular value decomposition. If no similar motif exists, a new motif is generated using the coordinates of this cluster. The cluster is oriented using the initial LAM alignment, where a rotation is created for the cluster that constrains the nearest neighbor atom to the z-axis and a second atom to the x-z plane. This process is then repeated for all the clusters associated with every atom in the model.

While the past LAM methods have used pre-defined rotations to orient the clusters, the least squares rotation now considers every atom in the cluster equally. Despite the Kabsch algorithm being known for decades, its implementation in processes such as the SLAM method is not trivial. The algorithm, more specifically, the singular value decomposition component requires a covariant matrix resulting from the matrix multiplication of atom positions of the cluster to atom positions of the motif. The order of atoms becomes crucial for the algorithm to succeed.

A complication that can arise is illustrated in figure 1. In this example a 2D rotation must be calculated to match the first cluster with points 1, 2 and 3 with the second cluster with points A, B and C. Applying the Kabsch algorithm in 2D with both clusters ordered alphanumerically, would fail since there is no possible rotation that can have points 1, 2 and 3 overlaid directly with points A, B and C respectively. Rather, the ideal rotation matrix would be solved when aligning points 1,3 and 2 to points A, B and C respectively. A straight forward solution would consider every permutation and apply the rotation that gives the best alignment. This brute force approach becomes impractical as the number of atoms in a cluster increases. Since the number of possible permutations is a factorial relationship with the number of atoms, coordinations that exist in metallic glasses would have billions to trillions of permutations for a single cluster. The vast majority of permutations would not enable a proper alignment by rotation.

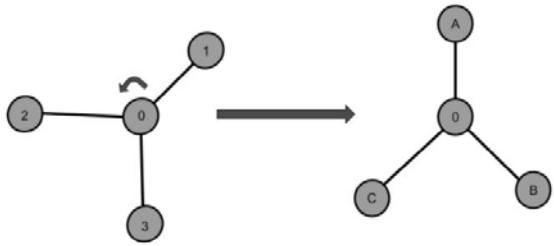

Figure 1: an example of a 2d rotation to map the cluster on the left to the cluster on the right. The ideal mapping is point 1 to A, point 2 to C and point 3 to B. Mapping point 2 to b would instead create a poor alignment.

In this new approach, broad attributes of the cluster are examined to filter out motifs significantly different from the cluster. The first and most trivial filter is coordination number. The remaining filters draw inspiration from the initial LAM method, where orientations were created by constraining two atoms. For every atom in the cluster, a bond angle distribution is created with the remaining cluster atoms. These distributions are sorted in ascending order and compared to the bond angle distributions of possible motifs. If a cluster is part of an existing motif, its bond angle distribution should be sufficiently similar to the motif's bond angle distribution. This filter alone is not enough to uniquely match a cluster to a single motif, so a third filter is applied.

In the third filter we effectively perform the initial LAM alignment. The relative atom used in the previous filter is chosen as the z-axis atom and the remaining atoms in the cluster are sampled as the x-z atom. To compare geometries, the positions of the atoms in the cluster are indexed to a cloud of points spaced around a sphere. A K-d Tree neighbor search matches each atom in a cluster to a point in this K-d cloud. The resulting list of indices contains orientational information in all three dimensions. These indices are compared to the corresponding indices of possible motifs. Similarity between the cluster and motif indices will indicate a potential match. This provides a means to map the atoms from the cluster to the target atoms of the motif, removing the need to sample many permutations.

With this coarse index comparison, it is possible a cluster could match a motif without being in an ideal alignment. At this point, we test the alignment of the cluster to the candidate motif and consider the least-squares difference between the aligned cluster and the motif. A minimum threshold is required to be considered a match that can be satisfied by multiple alignments. Minimizing the least-squares difference produces the rotation with the best alignment, classifying the cluster to be of that motif. In the event no candidate motif satisfies all three filters, a new motif is created using that cluster.

Through this geometric process, rotational information is preserved making all operations reversible and repeatable. In addition, 3D density maps can be readily reproduced using any cluster size without repeating the entire process.

DISCUSSION

Comparison of amorphous germanium

As a first test, we compare two established models of a-Ge. The first is a 100,000 atom, continuous random network (CRN) model [24] and the second a 100,000 atom model refined to high-resolution x-ray scattering data using Reverse Monte Carlo (RMC) [21]. In the case of the CRN model, the most dominant motif found through SLAMs is a slightly disordered tetrahedral structure, which describes 98.8% of the atoms in the model. This motif is shown in figure 2a. The remaining 1.2% of the CRN atoms

consists of highly disordered tetrahedra and some rare cases of atoms of coordinations other than four. This is consistent with observations by Tomberli et al. [21].

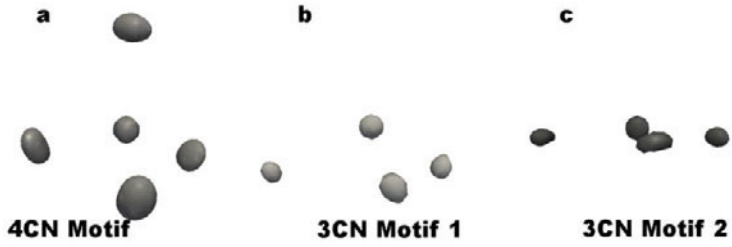

Figure 2: 3D density maps of motifs found in a-Ge. Figure a is the dominant 4-coordinated motif, figures b and c the two dominant motifs for 3-coordination in the RMC refined model. A small tilt can be seen to exist in the 4-coordinated motif and variations of buckling are apparent between the two 3-coordinated motifs.

Using the motifs found in the CRN model as a template, the SLAM method is applied to the RMC refined model of a-Ge. The refined model is composed of 65.5% 4-coordinated atoms and 27.5% 3-coordinated atoms. As expected, of the 4-coordinated atoms, the majority have the same motif described in figure 2a. Roughly 10% of the 4-coordinated atoms are disordered beyond what is described in this motif. Rahemtulla et al. [22] alluded to this observation, but could not resolve the additional motifs because the LAMs were dominated by the tetrahedral motif. The 3-coordinated atoms in the RMC refined model fall into two motifs. The dominant motif has 60% of the atoms in the buckled germanene-like 3-coordinated motif described by Tomberli et al. [21]. The remaining 40% of atoms are in a different motif with the center atom and its three nearest neighbor atoms coplanar as in graphene. Both of these motifs can be seen in figures 2b and 2c.

Application to $Cu_{50}Zr_{50}$ metallic glass

The self-sorting ability of SLAMs now enables quantitative and statistical comparisons that have existed in methods like Voronoi indexing, simultaneously enabling visual observations of asymmetries and perturbations from crystalline positions that would otherwise be impossible. To further test the functionality of SLAMs, this method is applied to a 300,000 atom model of $Cu_{50}Zr_{50}$ metallic glass [25]. In the analysis of metallic glasses, the common motifs expected to exist are the Kasper polyhedra, namely the Z10 bi-pyramid structure and the Z12 icosahedron [10,20]. The icosahedron is indeed observed and shown in figure 3a.

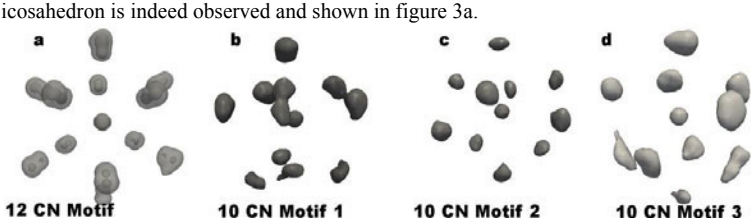

Figure 3: 3D density maps of dominant motifs in $Cu_{50}Zr_{50}$. Figure a, shows the icosahedral motif with additional contours showing the two possible radial positions that can be occupied. Figures b through d are the dominant 10-coordinated motifs in decreasing order. Figure d, follows a structure similar to the Z10 polyhedron, but is much more disordered.

The most striking observation for this 12-coordinated motif is the appearance of the double atom distribution at each site corresponding to the Cu-Cu and Cu-Zr bonds. The lack of an additional third atom distance consistent with a Zr-Zr bond is because Zr rarely appears in this icosahedral motif.

In the case of 10-coordination, the degree of ordering is much weaker. A subset of the dominant 10-coordinated motifs is shown in figures 3b through 3d. The most dominant motif describes a more complicated structure. The northern hemisphere appears to have 5-fold symmetry and is similar albeit a more disordered version of the icosahedron. The two remaining motifs shown in figures 3c and 3d depict structures tending towards the Z10 polyhedron. Motif-2 may be considered an intermediate between Motifs 1 and 3. Motif-3 exhibits the orientation expected in a Z10 polyhedron. This structure is relatively disfavored describing only 7.5% of the 10-coordinated atoms.

Upon applying Voronoi indexing to the clusters in these motifs, the limitations become apparent with Motifs 1, 2 & 3 being described by 710, 382, and 390 different sets of Voronoi indices respectively. A major contribution to this variance is the additional interaction of second shell atoms introducing additional facets. Removing these effects can trivialize the results with all 3 motifs containing upwards of 50% of the <0,2,8,0> Z10 Kasper polyhedron, with the remaining atoms distributed over 15 different sets of indices. A visual inspection of the three LAMs of figure 3 contradicts the strong presence of an ordered Z10 polyhedron that could be predicted through Voronoi analysis..

CONCLUSIONS

SLAM analysis on a-Ge shows 3-coordinated atoms are described by two distinct motifs. The tetrahedral-like structure is shown to be the motif of 90% of the 4-coordinated atoms, with the remaining atoms lacking this nearest neighbor ordering. The SLAM's ability to not only extract these unique motifs, but also the occupancy allows deeper and more quantitative comparisons. An examination of $Cu_{50}Zr_{50}$ metallic glass confirms the presence of icosahedral ordering, with SLAMs able to resolve the Cu-Cu and Cu-Zr bond length variances. The 10-coordinated motifs found deviate from the expected Kasper polyhedra. One motif was found to be similar the Z10 polyhedra, but much more disordered. Voronoi analysis fails to describe these structures with hundreds of different sets of Voronoi indices.

Models of amorphous solids are being proposed with goals of addressing ever more subtle structure effects such as slight changes in a-Ge upon annealing [26,27] to shear band formations in metallic glass [25]. The challenge remains to identify the structural features that characterize these differences. The categorizations coupled with the powerful visualization of SLAMs can enable a deeper means of probing perturbations, capturing changes in motifs as well as their relative distributions. All of which are likely to go unnoticed in traditional analysis.

References

[1] a. C. Wright and M.F. Thorpe, Phys. Status Solidi **250**, 931 (2013).
[2] T. Proffen, V. Petkov, S.J.L. Billinge, and T. Vogt, Zeitschrift Für Krist. - Cryst. Mater. **217**, 47 (2002).
[3] R.L.C. Vink, G.T. Barkema, W.F. Van der Weg, and N. Mousseau, J. Non. Cryst. Solids **282**, 248 (2001).
[4] D. Polk, J. Non. Cryst. Solids **5**, 365 (1971).

[5] F. Wooten, K. Winer, and D. Weaire, Phys. Rev. Lett. **54**, 1392
[6] (1985). K.B. Borisenko, B. Haberl, A.C.Y. Liu, Y. Chen, G. Li, J.S. Williams, J.E. Bradby, D.J.H. Cockayne, and M.M.J. Treacy, Acta Mater. **60**, 359 (2012).
[7] S. Trady, M. Mazroui, A. Hasnaoui, and K. Saadouni, J. Non. Cryst. Solids (2016).
[8] H.W. Sheng, W.K. Luo, F.M. Alamgir, J.M. Bai, and E. Ma, Nature **439**, 419 (2006).
[9] M.H. Bhat, V. Molinero, E. Soignard, V.C. Solomon, S. Sastry, J.L. Yarger, and C. a Angell, Nature **448**, 787 (2007).
[10] J. Zemp, M. Celino, B. Schönfeld, and J.F. Löffler, Phys. Rev. Lett. **115**, 1 (2015).
[11] Q. Yu, X.D. Wang, H.B. Lou, Q.P. Cao, and J.Z. Jiang, Acta Mater. **102**, 116 (2016).
[12] A.B. Cairns and A.L. Goodwin, Chem. Soc. Rev. **42**, 4881 (2013).
[13] D.R. Queen, X. Liu, J. Karel, H.C. Jacks, T.H. Metcalf, and F. Hellman, J. Non. Cryst. Solids **426**, 19 (2015).
[14] X. Liu, D.R. Queen, T.H. Metcalf, J.E. Karel, and F. Hellman, Phys. Rev. Lett. **113**, 1 (2014).
[15] S. Le Roux, V. Petkov, and IUCr, J. Appl. Crystallogr. **43**, 181 (2010).
[16] D. Faken and H. Jónsson, Comput. Mater. Sci. **2**, 279 (1994).
[17] P.J. Steinhardt, D.R. Nelson, and M. Ronchetti, Phys. Rev. B **28**, 784 (1983).
[18] Brostow W., M. Chybicki, R. Laskowski, and J. Rybicki, Phys. Rev. B **57**, 113448 (1998).
[19] T. Fukunaga, K. Itoh, T. Otomo, K. Mori, M. Sugiyama, H. Kato, M. Hasegawa, A. Hirata, H. Y., and A.C. Hannon, Mater. Trans. **48**, 1698 (2007).
[20] X.W. Fang, C.Z. Wang, Y.X. Yao, Z.J. Ding, and K.M. Ho, Phys. Rev. B - Condens. Matter Mater. Phys. **82**, 1 (2010).
[21] B. Tomberli, A. Rahemtulla, E. Kim, S. Roorda, and S. Kycia, Phys. Rev. B **92**, 64204 (2015).
[22] A. Rahemtulla, B. Tomberli, and S. Kycia, J. Appl. Crystallogr. (2018).
[23] W. Kabsch and IUCr, Acta Crystallogr. Sect. A **32**, 922 (1976).
[24] G.T. Barkema and N. Mousseau, Phys. Rev. B **62**, 4985 (2000).
[25] A.R. Hinkle, C.H. Rycroft, M.D. Shields, and M.L. Falk, Phys. Rev. E **95**, 53001 (2017).
[26] K. Laaziri, S. Kycia, S. Roorda, M. Chicoine, J.L. Robertson, J. Wang, and S.C. Moss, Phys. Rev. Lett. **82**, 3460 (1999).
[27] S. Roorda, C. Martin, M. Droui, M. Chicoine, a. Kazimirov, and S. Kycia, Phys. Rev. Lett. **255501**, 1 (2012).